

# Scalable Compact Models for Embedded Passives

Kok-Yan Lee<sup>1</sup>, Saeed Mohammadi<sup>2</sup>, Pallab K. Bhattacharya<sup>1</sup> and Linda P. B. Katehi<sup>2</sup>

<sup>1</sup>University of Michigan, EECS, 1301 Beal Avenue, Ann Arbor, MI 48109, (1)734-763-6678, pkb@eecs.umich.edu

<sup>2</sup>Purdue University, ECE, West Lafayette, IN 47907, (1)765-494-3557, saeed@purdue.edu

**Abstract**— This paper presents a new comprehensive methodology for the development of scalable models for embedded passives. These models are derived from fundamental lossy transmission line theory. Using Taylor's series and continued fractions approximation, very accurate second and third order intrinsic capacitor and inductor models have been demonstrated. With the second order model, we are able to match the measured response up to the first resonance frequency. With the third order models, we are able to match the measured response beyond the first resonance frequency. The wideband accuracy provided by the third or higher order intrinsic models are necessary in transient and harmonic frequency analysis. The parameter extraction does not require any optimization and is accurate and unambiguous. The third order continued fractions model, introduced in this paper, matches the frequency dependent non-linear effects observed in the passives without a need for frequency dependent elements.

## I. INTRODUCTION

There are many publications related to developing models for capacitors and inductors [1]–[5], but there are much fewer work that is related to wide-band behavior of on-chip and embedded passives. A model based on a simple transmission line model without any substrate effects was mentioned by Pucel [6]. Most recently, the conventional  $\pi$ -model was extended with frequency dependent lumped elements [2], [3] which does a better job of describing the higher order frequency effects, but prevents integration of the model with time domain simulators. There are also alternative models such as distributed models and other lumped models that try to address the high frequency effects [4], [5].

This paper presents a new modeling methodology for passives based on fundamental lossy transmission lines. The model is scalable from narrow-band to wide-band depending on the accuracy required and is, to the authors' knowledge, the first model that systematically matches the passive component response beyond the first resonance without need for optimization. During the model development, we will show that the frequency dependent nonlinear effects are taken care of naturally by the continued fractions model using only ideal frequency independent elements that is amenable to time-domain transient analysis or harmonic balance nonlinear simulation. We will also show how to reliably, quickly and unambiguously extract the model parameters without requiring optimization.

## II. MODEL DEVELOPMENT

Our model development starts with the standard  $\pi$  model for the passive component, with input and output extrinsic shunt capacitances and intrinsic series reactive impedance as shown in Fig. 1(a).

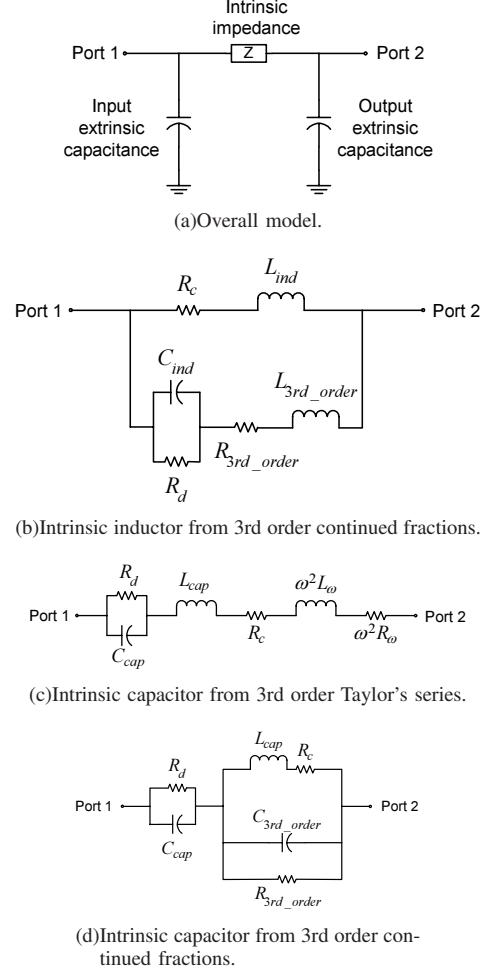


Fig. 1. Equivalent circuit model of passives.

### A. Extraction of the extrinsic capacitances and intrinsic impedance

The input and output extrinsic shunt admittances and the intrinsic series impedance are extracted from the measured two-port  $S$  parameters. Knowing the  $S$  to  $ABCD$  transform equations, and the  $ABCD$  matrix for the series intrinsic capacitor or inductor impedance,  $Z_{cap}$  or  $Z_{ind}$ , and the  $ABCD$  matrix for the shunt extrinsic admittance,  $Y_{ext}$ , gives us the means to obtain the intrinsic inductances and capacitances and the extrinsic capacitances unambiguously, to the extent where we can differentiate the port 1 and port 2 extrinsic capacitances. The resultant equations are:

$$Z_{ind/cap} = B_{total} \quad (1a)$$

$$Y_{ext1} = \frac{D_{total} - 1}{B_{total}} \quad (1b)$$

$$Y_{ext2} = \frac{A_{total} - 1}{B_{total}}. \quad (1c)$$

### B. Intrinsic Inductor Model

The intrinsic inductor is modeled as a transmission line with an ideal short-circuit at the end. This equation is then approximated using the first, second and third order continued fractions approximation of  $\tanh(\gamma l)$  and translated into traditional equivalent circuits to obtain our first, second and third order intrinsic inductor models. The model could easily be extended further to a fourth order if necessary to model the inductor to the second resonance. Using an ideal short circuit termination, the resulting transmission line equation is

$$Z_{ind} = Z_0 \tanh(\gamma l). \quad (2)$$

The result of (2) is not translatable into a traditional equivalent circuit. Using the continued fractions approximation of  $\tanh(\gamma l)$  given by

$$\tanh(\gamma l) = \frac{(\gamma l)}{1 + \frac{(\gamma l)^2}{3 + \frac{(\gamma l)^2}{5 + \dots}}} \quad (3)$$

allows for very simple translation into equivalent electrical circuits. The residual errors for these circuit models can be considered by computing the error between the model and the measured data. Using the above equations, we are able to obtain the first, second and third order approximation of the intrinsic inductor input impedance,  $Z_{ind}$ . The third order equivalent model is shown in Fig. 1(b).

### C. Intrinsic Capacitor Model

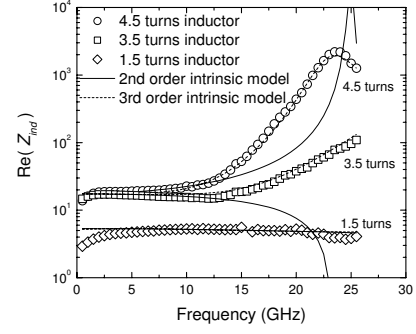
The intrinsic capacitor is modeled as an ideal transmission line with an ideal open-circuit. Using Taylor's series approximation and the continued fractions approximation, as described in Section II-B, we translate the derived mathematical equation into conventional equivalent electrical circuit. As in Section II-B, the third order equivalent circuit model for the capacitor is determined as shown in Fig. 1(c) and Fig. 1(d). With the Taylor's series model, the frequency dependent resistor is needed for modelling the capacitor, while the continued fractions model is able to handle the frequency dependence without resorting to frequency dependent components. This is shown in Fig. 7

## III. PARAMETER EXTRACTION

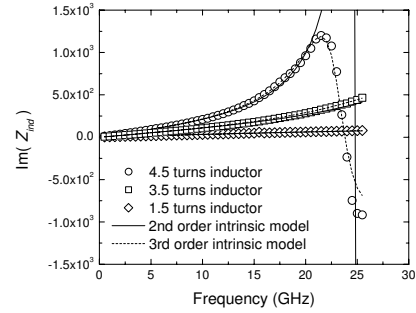
In this section, we will demonstrate the parameter extraction for a number of integrated inductors and capacitors using their measured  $S$  parameters. Specifically we measured three different spiral inductors (with one and a half turns, three and a half turns and four and a half turns), and three different MIM capacitors with areas of:  $1000 \mu\text{m}^2$ ,  $3000 \mu\text{m}^2$  and  $6000 \mu\text{m}^2$ .

### A. Inductor Model

To obtain all the model parameters for the second order and third order intrinsic inductor impedance without optimization, both the real and imaginary part of the input admittance of the second order intrinsic inductor model are approximated by linear equations, assuming that  $(\omega L_{ind}/R_c)^2 \gg 1$ . The parameters extracted for the second order model are then used to calculate the parameters of the third order model.



(a)Real.



(b)Imaginary.

Fig. 2. Comparison between the intrinsic inductor and the second and third order models.

This allows us to cast the resultant intermediate equations as straight lines with the assumption that  $(\omega R_d C_{ind})^2 \gg 1$ , thus allowing us to extract the third order model parameters.

Fig. 2(b) and Fig. 2(a) show the imaginary and real data match between the second order and the third order intrinsic inductor model and the measured data. We note that the third order model is generally more accurate and able to match the data at higher frequencies. The only exception is for the one and a half turn inductor, where both the second and third order model gives generally similar results. This is due to the fact that the one and a half turn inductor has not reached resonance yet within the measurement frequency range. This indicates that a second order model is good enough to match the one and a half turn inductor. Fig. 3 shows the complete equivalent circuit model of the inductor.

### B. Capacitor Model

In the case of the intrinsic capacitor, we found that the second order model is as accurate as the third order models for the imaginary part. However, the second order model is not as accurate at higher frequencies for the real part.

Fig. 4 shows the complete equivalent circuit model of the capacitor and Fig. 5 and Fig. 6 show the real and imaginary data match between the measured  $Y_{11}$  and the model for a  $1000 \mu\text{m}^2$ ,  $3000 \mu\text{m}^2$  and  $6000 \mu\text{m}^2$  capacitors. Fig. 7 shows the input quality factor,  $Q_{11}(\omega)$  for a single  $6000 \mu\text{m}^2$  capacitor. Notice that both of the third order models, the frequency independent continued fractions model and the frequency dependent Taylor's series model, matches the measured data

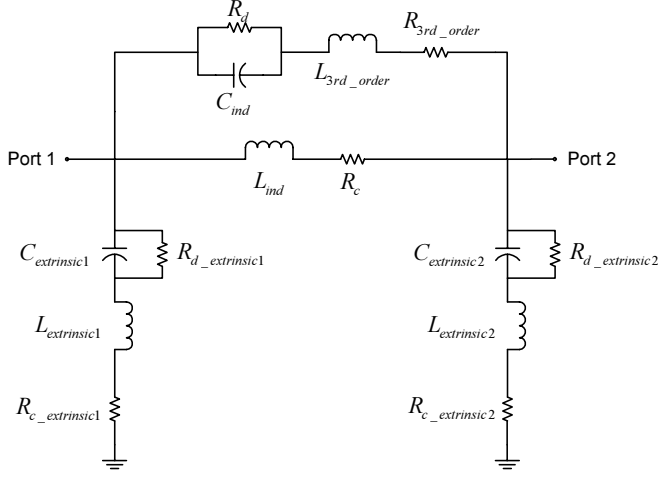


Fig. 3. Complete Inductor model.

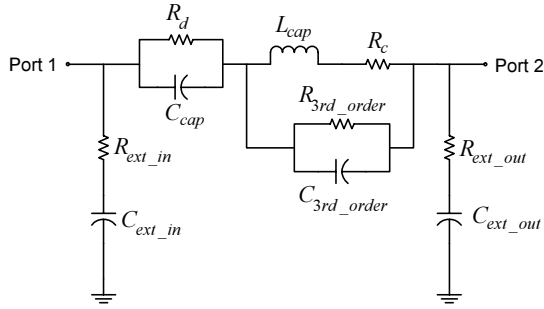


Fig. 4. Complete capacitor model.

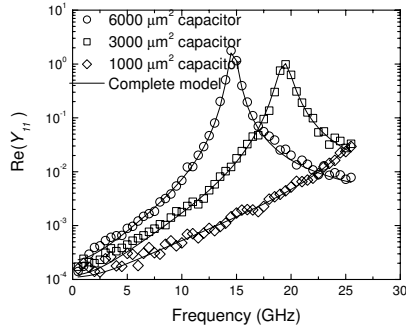


Fig. 5. Comparison of the measured and modelled  $\text{Re}(Y_{11})$ .

beyond the first resonance. While the second order model is only able to match the measured data to first resonance.

#### IV. CONCLUSION

In conclusion, we have demonstrated a new modeling methodology for integrated passives based on fundamental transmission line theory and continued fractions approximation. This model is scalable depending on the accuracy required. The third order model is, to the authors' knowledge, the first reported model that is able to match the measured results beyond the first resonance in a systematic fashion. The wide-band accuracy provided by the third or higher order intrinsic model is needed in transient response design and also in designs where the harmonic frequency response is important.

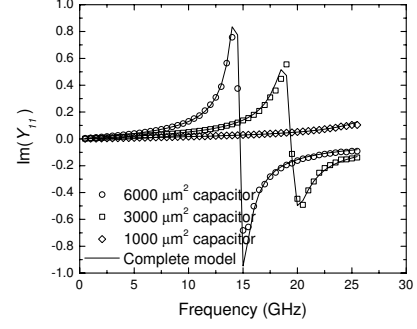


Fig. 6. Comparison of the measured and modelled  $\text{Im}(Y_{11})$ .

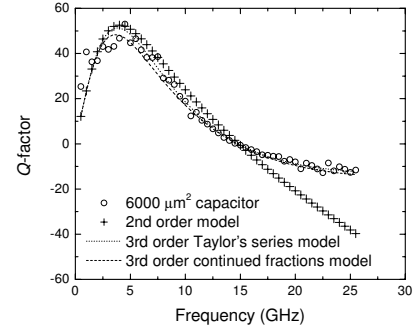


Fig. 7. Comparison of the  $6000\mu\text{m}^2$  capacitor's measured and modelled input quality factor,  $Q_{11}(\omega)$ .

The parameter extraction does not require any optimization and is accurate and unambiguous.

#### REFERENCES

- [1] N. M. Nguyen and R. G. Meyer, "Si ic-compatible inductors and lc passive filters," *IEEE Journal of Solid State Circuits*, vol. 25, no. 4, pp. 1028–1031, Aug. 1990.
- [2] E. Pettenpaul, H. Kapusta, A. Weisgerber, H. Mampe, J. Luginsland, and I. Wolff, "Cad models of lumped elements on gaas up to 18 ghz," *IEEE Transactions on Microwave Theory and Techniques*, vol. 36, no. 2, pp. 294–304, Feb. 1988.
- [3] J. N. Burghartz, M. Soyuer, and K. A. Jenkins, "Microwave inductors and capacitors in standard multilevel interconnect silicon technology," *IEEE Transactions on Microwave Theory and Techniques*, vol. 44, no. 1, pp. 100–104, Jan. 1996.
- [4] J. R. Long and M. A. Copeland, "The modeling, characterization, and design of monolithic inductors for silicon rf ic's," *IEEE Journal of Solid-State Circuits*, vol. 32, no. 3, pp. 357–369, Mar. 1997.
- [5] T. Kamgaing, T. Myers, M. Petras, and M. Miller, "Modeling of frequency dependent losses in two-port and three-port inductors on silicon," *2002 IEEE Radio Frequency Integrated Circuits Symposium*, pp. 307–310, 2002.
- [6] R. A. Pucel, "Design considerations for monolithic microwave circuits," *IEEE Transactions on Microwave Theory and Techniques*, vol. 29, no. 6, pp. 513–534, June 1981.

